J. Astrophys. Astr. (2023) 44:24
https://doi.org/10.1007/s12036-023-09911-5

ORIGINAL RESULTS

Detecting global signal from cosmic dawn and epoch of reionization with SKA

MAYURI SATHYANARAYANA RAO[1,*], N. UDAYA SHANKAR[1], RAVI SUBRAHMANYAN[2] and SAURABH SINGH[1]

[1]Astronomy and Astrophysics, Raman Research Institute, Bangalore 560080, India.
[2]Space and Astronomy CSIRO, 26 Dick Perry Ave., Kensington, WA 6151, Australia.
*Corresponding author. E-mail: mayuris@rri.res.in

MS received 14 March 2022; accepted 31 October 2022

Abstract. A key science project for SKA-Low is the interferometer imaging of spatio-temporal fluctuations in the hydrogen ionization fraction and spin temperature as a diagnostic of cosmic dawn (CD) and epoch of reionization (EoR) in the redshift range $6 \lesssim z \lesssim 28$. However, detection of the global CD/EoR signal, which provides the differential HI 21-cm brightness temperature with respect to the background radiation temperature, is outside the current purview of SKA-Low observing in interferometer mode. This global CD/EoR signal can provide the critical zero-spacing measurement vital for establishing the base level of fluctuations measured by SKA-Low interferometers. We present here, a concept to detect the global CD/EoR signal as a supplement to the CD/EoR key science of SKA-Low. This would be enabled by adding a compact array of outrigger antennas interspersed between the core stations of SKA-Low. The autocorrelations of the outrigger antennas would form the measurement set for the global CD/EoR. The visibilities measured between outriggers and SKA stations would be 'blind' to the global CD/EoR signal and would provide a Global Sky Model and calibration of the bandpass and mode-coupling in the primary beam of the outriggers. The global signal measurement capability will strengthen the SKA-Low CD/EoR program.

Keyword. Cosmology: dark ages, reionization, first stars—instrumentation: interferometer—telescopes.

1. Introduction

All ongoing experiments to study the cosmic dawn (CD) and epoch of reionization (EoR) using the redshifted 21-cm signal of neutral hydrogen as a probe, follow one of two approaches: power-spectrum measurement studies (Madau *et al.* 1997; Morales & Wyithe 2010; Fialkov & Barkana 2014) and global CD/EoR signal detection (Furlanetto *et al.* 2006; Pritchard & Loeb 2012). Instruments, such as uGMRT (Pal *et al.* 2021), MWA (Yoshiura *et al.* 2021), LOFAR (Mertens *et al.* 2020) and HERA (Abdurashidova *et al.* 2022) adopt the former approach. At the same time, several other ongoing experiments employ the latter, such as the Shaped Antenna measurement of the background RAdio Spectrum (SARAS) (Singh *et al.* 2022), Experiment to Detect the Global Epoch-of-Reionization Signature (EDGES) (Bowman *et al.* 2018), Cosmic Twilight Polarimeter (CTP) (Nhan *et al.* 2019), Radio Experiment for the Analysis of Cosmic Hydrogen (REACH) (de Lera Acedo 2019) and Large-Aperture Experiment to Detect the Dark Ages (LEDA) (Bernardi 2017). A key science goal of the SKA-Low is: Probing the Dark Ages: Cosmic Dawn and the Epoch of Reionization, by adopting power spectrum measurement as the tool of choice (Mellema *et al.* 2013). The large collecting area of the SKA-Low and the resulting improvement in sensitivity will allow the SKA-Low to not only measure the EoR power-spectrum, but also directly image the spatio-temporal fluctuations in the HI differential brightness temperature (Koopmans *et al.* 2015). However, detecting the global CD/EoR signal is outside the purview of SKA-Low. In this paper, we propose a method to enhance the SKA's capability to also measure the global CD/EoR signal, thus, combining both the above approaches in one instrument. In Section 2,

This article is part of the Special Issue on "Indian Participation in the SKA".

Published online: 28 March 2023

we provide a brief description of the global signal. In Section 3, we discuss the motivation for global signal detection (co-located) with the SKA-Low along with its interferometric mode of operation. General design principles for a clean signal detection that motivate engineering changes in the SKA-Low for the same are listed in Section 4. In Section 5, we suggest three possible strategies to implement such a capability. Our preferred mode of implementing global CD/EoR signal detection by using an array of outrigger antennas with SKA-Low is further described in Section 6, with a minimum checklist to implement the same listed in Section 7. We also briefly discuss detecting yet another global cosmological signal—primordial recombination lines—with SKA-Mid in Section 8. Following a summary in Section 9, we end with some closing remarks regarding global CD/EoR signal detection in Section 10.

2. Global signal from CD and EoR

Hydrogen gas makes up to ∼75% of the mass of the baryons in the Universe. This makes atomic hydrogen an ideal tracer of the history and evolution of the Universe over cosmic time (McQuinn 2016). This section presents a brief overview of the physics affecting hydrogen over cosmic time. We refer the readers to the numerous useful reviews on this topic for the details, including Zaroubi (2013). Following big bang nucleosynthesis, baryonic matter is comprised primarily of ionized hydrogen (protons), helium nuclei and electrons. These are tightly coupled to radiation or photons. As the Universe expands and cools, ionized helium (He III) with its higher binding energy, recombines to He II (at $z \sim 5000$–8000) and then to He I (at $z \sim 1600$–3500). At a redshift of $z \sim 1100$, hydrogen recombines, leading to the physical decoupling of the photons from baryons. From that point on, the majority of photons free stream without scattering till the present day, where they appear as the relic cosmic microwave background (CMB). Although photons decouple from the baryons at $z \approx 1100$, the large photon–baryon ratio ($\sim 10^9$ photons per baryon) means that scattering of photons from the small residual ionized fraction of free electrons ($x_e \sim 10^{-4}$) (Seager *et al.* 2000) maintains thermal equilibrium between free electrons and the CMB (Peebles 1993). Collisions between free electrons and the remainder of the baryons maintain $T_K = T_{\rm CMB}$, where T_K is the kinetic gas temperature and $T_{\rm CMB}$ denotes the CMB temperature. This thermal coupling eventually ends at a redshift of $z \sim 200$ as dilution of the gas and CMB density with Hubble expansion reduces the photon–electron scattering rate below a critical threshold. With thermal decoupling, the gas begins to cool adiabatically with expansion, and its temperature scales as $T_K \propto (1+z)^2$, cooling faster than the CMB, which evolves as $T_{\rm CMB} \propto (1+z)$. For the first time in the Universe's evolution, there exist two separate temperature scales that dictate the level populations in the atomic gas, namely, kinetic gas temperature and CMB temperature. This temperature difference creates the opportunity for an interesting 21-cm signal. Key to understanding the 21-cm signal is the evolution of the spin temperature T_s, which describes the ratio of atoms in the upper and lower hyperfine levels,

$$\frac{n1}{n0} = 3{\rm e}^{-T_*/T_s},$$

where $T_* \equiv (hc)/(k\lambda_{21\ {\rm cm}}) = 0.068$ K (Field 1959). The spin temperature is set by the relative rate of spin-flip transitions driven by interaction with CMB photons scattering off Ly-α photons, or collisions between the mix of neutral hydrogen atoms, free protons and free electrons. Formally it is determined by:

$$T_s^{-1} = \frac{T_{\rm CMB}^{-1} + x_\alpha T_\alpha^{-1} + x_c T_c^{-1}}{1 + x_\alpha + x_c}, \tag{1}$$

where T_α is the color temperature of the Ly-α radiation field at the Ly-α frequency and x_c, x_α are coupling coefficients due to atomic collisions and scattering off Ly-α photons, respectively (Field 1958). T_α is closely coupled to T_K by recoil during repeated scattering and the spin temperature becomes strongly coupled to the gas temperature when $x_{\rm tot} \equiv x_c + x_\alpha \gtrsim 1$. In the linear limit of low optical depth, combining the spin temperature with the amount of neutral hydrogen, which is parametrized by the neutral fraction $x_{\rm HI}$ (ignoring the overdensity and peculiar velocity terms for the global signal) gives the differential brightness temperature:

$$\delta T_{\rm b}^{\rm obs}(\nu) \approx 27 x_{\rm HI} \left(\frac{\Omega_{\rm b} h^2}{0.022}\right) \left(\frac{0.15}{\Omega_{\rm m} h^2} \frac{1+z}{10}\right)^{\frac{1}{2}} \times \left(\frac{T_s - T_{\rm R}}{T_s}\right) {\rm mK}. \tag{2}$$

We note that recent work by Datta *et al.* (2022) shows that in conditions expected to prevail during CD, the optical depth to 21-cm radiation is large, and that the linear approximation in Equation (2), overestimates the spin temperature by 5% in standard models. Working chronologically down from high redshift, we first see a 21-cm absorption signal during the cosmic dark ages. In the absence of exotic new physics, the evolution of this signal is determined by collisional coupling and the effect of adiabatic expansion on the temperature of the

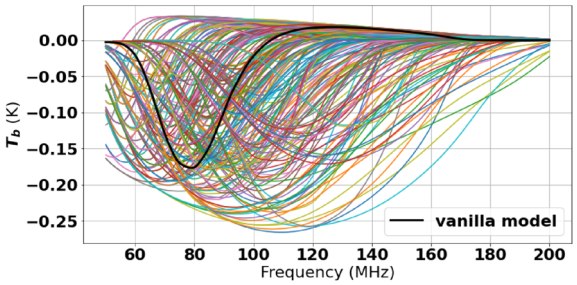

Figure 1. A non-exhaustive atlas of plausible global redshifted 21-cm signatures of CD/EoR allowed by standard models. Data courtesy: Cohen *et al.* (2017).

gas. However, it is possible that exotic physics and dark matter annihilation, for example, can heat the gas in this early phase and changing this picture. More generically, the collisional coupling becomes ineffective as the gas becomes more diffuse and cooler and it is only when the first stars and galaxies form the 21-cm signal becomes complex. Galaxies produce Ly-α photons that couple $T_s \sim T_K$, leading to the second absorption feature at redshifts less than about 30 (Wouthuysen 1952). The start of this potentially deep second absorption feature occurs as Ly-α coupling starts, and the end is governed by the eventual heating of the Universe by UV and soft X-rays, which leads to the final emission feature (Pritchard & Loeb 2008). Ultimately, the gas is likely to enter a hot, Ly-α coupled state where $T_s \gg T_{\rm CMB}$, although this is not guaranteed. This saturates the all-sky 21-cm signal removing any dependence on T_s, so that δT_B is entirely determined by the mean density and neutral fraction $x_{\rm HI}$. As ionizing UV photons from star-forming galaxies reionize the Universe, the neutral fraction $x_{\rm HI}$ falls to zero (McGreer *et al.* 2015). This is the final emission feature of the all-sky 21-cm signal, whose decline indicates the progression of reionization.

The details of the astrophysics (e.g., $x_{\rm HI}$, spectral energy distribution of the first sources) and cosmology (such as total matter density and total baryon density) determine the amplitude and shape (turning points) of the global CD/EoR signal (Pritchard & Loeb 2010). Figure 1 shows a range (non-exhaustive set) of global CD/EoR signals predicted by standard models, suggesting that the parameter space is wide open (Cohen *et al.* 2017). Hence a definitive detection of this signal will enable determining the details of the physics of the Universe over CD/EoR.

3. Scientific motivation

As would be measured by SKA-Low, the evolving CD/EoR power spectrum is a manifestation of ionizing sources' spatial distribution and the gas's density structure. Both are consequences of the dynamical and astrophysical evolution in the matter distribution power spectrum, and these result in spatial structure in hydrogen spin temperature and ionization fraction. SKA-Low observations in interferometer mode would measure the power spectrum of brightness temperature fluctuations about the evolving mean all-sky absorption or emission signature. However, in this mode, the critical zero spacing measurement of reionization fluctuations, which is vital for establishing the base level of the interferometer measurement of fluctuation power, is missing (Liu & Parsons 2016). SKA-Low interferometers are, unfortunately, 'blind' to this critical global CD/EoR signal. This all-sky CD/EoR signal, is a direct measure of the mass-averaged evolution in the state of the gas, and cleanly establishes whether the interferometer measurements of fluctuating power at any epoch refer to absorption or emission. Therefore, measuring the global CD/EoR signal is critical for a complete understanding of the physics of CD/EoR. Such a measurement would provide significant value addition to the science returns of the SKA-Low key science project: Probing the Dark Ages: Cosmic Dawn and the Epoch of Reionization.

Since current observations poorly constrain the astrophysics of CD/EoR, substantial uncertainty exists in our knowledge of the redshifts at which 21-cm power might be detectable. An independent and early detection of the all-sky signature of cosmic evolution in the gas is advantageous and it aids in selecting optimum bands for SKA-Low imaging of the evolving power spectrum and selecting control bands, where the power is expected to be diminished. Therefore, SKA-Low measurements of the global CD/EoR signal are to be viewed as an essential precursor to detection and imaging of spatio-temporal 21-cm power and a necessary and supplementary zero-spacing measurement that provides the base level over which the fluctuation power resides. Several ongoing and proposed experiments aim to make precision measurements of the spectrum of the cosmic radio background to detect the global CD/EoR signal. So the question arises as to why we even consider all-sky measurements with SKA-Low when dedicated purpose-built single-element spectral radiometers might suffice! Arguments supporting global CD/EoR signal detection with SKA-Low in addition to its interferometric imaging mode are given below:

- Precise mode-coupling and receiver bandpass calibration: A significant challenge facing

ongoing total power spectral radiometer experiments to detect the global CD/EoR signal is the modulation of the spectral response of the radiometers by the spectral gains of the antennas and receiver electronics (Bernardi *et al.* 2015). Additionally, depending on the magnitude of the dependence of the antenna beam pattern on frequency, the response contains spectral structure arising from the coupling of structure in the continuum brightness distribution to the frequency domain (Singh *et al.* 2018). SKA-Low in interferometer mode solves simultaneously for the brightness distribution of the sky (called the Global Sky Model) and the beam patterns of the interferometer elements. It hence provides precise calibration solutions for the mode-coupling and receiver bandpass.

- RFI mitigation: Yet another challenge facing global CD/EoR experiments is the detection and mitigation of Radio Frequency Interference (RFI). The detection and mitigation of RFI will be far superior in measurements that simultaneously record autocorrelation and cross-correlation spectra, as would be possible with the strategies discussed herein. For example, Stokes V visibilities constitute a sensitive calibration set for RFI recognition in time-frequency space and can effectively reject RFI-corrupted autocorrelation spectra (Offringa *et al.* 2010).
- Wide bandwidth: Most global CD/EoR experiments operate in relatively narrow bandwidths of an octave or lower, and hence, probe relatively thin and often non-contiguous slices of redshifts over which the CD/EoR spectral signal spans. When observing over the bands exceeding an octave, the design of antennas with frequency-independent beam patterns at the precision required to avoid mode coupling is a formidable challenge. The substantial collecting area and hence, sensitivity in baselines with numerous SKA-Low stations provide an opportunity for precise mode coupling calibration via solving for both element beam patterns and sky models using interferometer visibilities. This allows relaxation of the precision required in the design specifications for the frequency-independent antennas whose autocorrelation spectra are to provide global CD/EoR measurements. With this relaxation, both the power spectrum and global CD/EoR signal measurements may be made using SKA-Low over the entire frequency range spanned by the EoR astrophysics. The SKA-Low band covers well over two octaves (50–350 MHz). If also used to detect the global CD/EoR signal, the SKA-Low would be the only instrument capable of measuring both the power-spectrum and global CD/EoR signal over contiguous wide bandwidths, thus providing a complete science data set for the CD/EoR key science project.

4. Design principles for all-sky CD/EoR observations

In measuring the all-sky spectrum of the cosmic radio background to detect the faint reionization signatures embedded therein, the effective collecting area of the sensor of the sky radiation is not of consequence. What is needed, is a spectral radiometer that may be precisely calibrated and a sensor that is ideally frequency-independent, so that sky brightness distribution of spatial structures do not result in confusing the spectral structure in the measurement set.

The cosmological signal is embedded in a foreground that is expected to be smooth. The foreground spectrum is a summation over numerous sources in the antenna beam pattern and along the line of sight. Each of these sources has a spectrum close to a power law, but may have a spread in their indices. The foreground spectrum would, therefore, be smooth likely described by a maximally smooth function of sufficiently high order for precise modeling (Sathyanarayana Rao *et al.* 2017). The cosmological signal in the total observing band must be indescribable as a maximally smooth function and hence, separable from the foregrounds. Thus, the observing band must necessarily include multiple turning points of the predicted reionization signature to distinguish it from smooth foregrounds. The expected cosmological signatures from CD and EoR are rather wideband signals, and hence, separation of the cosmological signal from foregrounds requires observing with bandwidths that are exceeding an octave.

The spectral response of any total power spectral radiometer contains the radio background spectrum modulated by the spectral gains of the antenna and electronics. The response includes additive terms from ohmic losses in the antenna and its interconnection to amplifier devices, amplifier noise, ground spillover, etc., (Meys 1978). Depending on the magnitude of dependence of the antenna beam pattern on frequency, the

response also contains spectral structure arising from mode coupling of sky structure into spectral structure. Over observing bands exceeding an octave, design of antennas with frequency-independent beam patterns to required precision (to avoid mode coupling) is challenging.

Experiments to date with single radiometers (antenna elements) have shown that the calibration of additive bias in the auto-correlation data is challenging, and many methods have been proposed for their marginalization. The additive contributions to autocorrelation spectra arise from ground spillover, antenna and balun ohmic losses, losses in the analog electronics signal path and amplifier noise, which have components that propagate along and against the nominal signal flow direction (such as those resulting from impedance mismatches between electronics in the signal path). Therefore, these system temperature components appear in the spectra of measurement sets with frequency structure due to the detector's multi-path propagation. The marginalization of additive bias requires special calibration techniques; some methods are discussed and demonstrated in designs of EDGES (Monsalve *et al.* 2017) and SARAS (Nambissan *et al.* 2021). Possible solutions include restricting path lengths for multi-path propagation by, for example, integrating high-gain amplifiers with baluns at the antenna terminals and optically isolating this front-end electronics from the rest of the receiver. Calibration of the response to amplifier noise requires the amplifier noise figure be switchable between high and low states. A differential response would provide the response to the amplifier noise. An alternate method that has been explored is including a bidirectional coupler with the amplifier so that a calibration noise may be injected at the same point in the signal path to measure the spectrometer response to a bidirectional noise that originates at the amplifier.

SARAS has led the way in demonstrating the value of correlation receivers that yield difference measurements between sky spectra and an internal reference load. Switching in the correlation receiver cancels many internal systematics and additive contaminants downstream of the switch. The correlation receiver provides complex spectra in which the sky power is exclusively in the real part following bandpass calibration, and the additive contaminants from receiver noise appear in real and imaginary parts with quadrature phase offset allowing for modeling and marginalization of their effects. Switching of the internal load provides a means for separating its contribution.

5. Observing all-sky cosmological signals with the SKA

The plan for SKA-Low in phase 1 is to comprise 512 stations, each containing 256 log-periodic dual-polarized antenna elements evenly distributed in an irregular-random configuration within a station diameter of 35 m. The stations are distributed in an array configuration in a large core with 75% antennas within a 2 km radius, and the remaining 25% in three spiral arms that give maximum baseline of 65 km. The array will operate from 50 to 350 MHz. All of the 256 log-periodic dipoles in each station are usually combined in a beam former and the dual polarization signals from 512 stations will be transported to a central signal processing building, where they will be channelized and cross-correlated to provide full Stokes measurements of the spectral visibilities. The station beams, when formed from all 256 elements, expose a field-of-view defined by a beam of 5° at the half-power points, at 100 MHz, which is expected to be circularly symmetric towards the zenith.

The CD and EoR signatures are from ∼40 to ∼200 MHz, almost entirely in the band of SKA-Low phase 1. We suggest three different and alternate approaches in generating the basic measurement sets for the all-sky CD/EoR signal using SKA-Low. They are:

1. to use as basic elements, the 35 m diameter stations configured as phased arrays of the 256 dipoles, (or)
2. to derive the sky signal by enabling just one log-periodic element in each station, (or)
3. to add, as an outrigger to each station, an antenna element with precision calibration capability that would provide the autocorrelation spectra.

We refer the reader to Subrahmanyan *et al.* (2015) for some additional discussions and strategies to detect the global 21-cm signal from CD/EoR with the SKA. Critical to the science is the calibration of the realized total-power spectral radiometers, in any of the strategies above. Calibration consists of: (a) determining the instrument bandpass for the sky signal, (b) modeling the additive spectral contamination from other sources of system noise: receiver noise, ground spillover, etc., and (c) correcting the measurement set for mode-coupling. The interferometer visibility measurements form the calibration set that generates all-sky model of the sky brightness distribution, while simultaneously solving for a model of the antenna pattern and the interferometer element bandpass and gains. These provide the bandpass for the sky signal in the station-based total power

radiometers (strategy 1) and also provide model of the mode coupling of sky structure into the spectral structure. Certain additive contaminants (receiver noise, etc.) require unique and separate calibration via the engineering design of the interferometer elements.

In all the three approaches, the observing strategy is to measure the autocorrelations of both polarization signals (X and Y) from each of the stations—to serve as the measurement set—and also full Stokes correlations (XX, YY, XY and YX) between all pairs of station signals to serve as the calibration set. This may be done for only signals from stations in the central core. An obvious advantage of restricting EoR all-sky measurements to the core stations is that this restricts the baselines used to those not severely affected by ionosphere; therefore, element gains, phases and bandpass calibrations may be derived with greater accuracy. The SKA-Low correlator is required to be configured to generate the total power autocorrelation spectra for the station signals from the central core, as well as the usual interferometer cross correlations. It may be noted here that the overhead to generate the autocorrelations is relatively small, and the autocorrelations may be performed by the resources freed by omitting the correlations between station signals from the outer arms.

5.1 *Strategy 1*

Strategy 1 is to phase an entire SKA-Low station to form a single element for the total power detection. Ideally, this strategy requires designing all log-periodic dipoles to have additive terms that are smooth functions of frequency that are separable from EoR signatures, which have turning points. Nonetheless, this strategy has the highest collecting area per station and hence, maximum sensitivity in baselines. Consequently, this method has minimum calibration errors and produces the best Global Sky Model. It may be noted here that enabling recording of accurate and useful auto-correlation spectra from these station signals is critical to using their sky-scans to provide the short and zero-spacing information, which will be vital for making complete and absolutely-calibrated Global Sky Models. No doubt, this is important for Galactic and Extragalactic science. From the perspective of all-sky EoR science, making an excellent Global Sky Model with all sky-structure modes represented is critical to subtracting the spectral structures in auto-correlation spectra arising from mode coupling, which is the spectral confusion due to any chromatic variation in the beam that would couple foreground structure to spectrum. However, the station beams are inevitably frequency-dependent. A frequency-dependent weighing of the element voltages prior to combining to form the station beams could potentially reduce the frequency dependence of the station beams, but not precisely because the elements do not provide continuous coverage of the aperture field. Along with interferometer solutions for the bandpass of the station beams, the models also provide calibrations for the mode coupling.

5.2 *Strategy 2*

Since collecting area is inconsequential for the all-sky signals, and simplicity and frequency invariance in the beam pattern is critical; the measurement set for the reionization signature may be derived using the sky signal from just one log-periodic antenna in each station of SKA-Low. In this case, just the station array element may be outfitted with electronics for calibration of its auto-correlation spectra. This method would also suffer mode-coupling owing to the frequency dependence in the beam (by definition, the antenna is log-periodic, which implies that it has periodic structure in antenna characteristics in log-frequency space). In this method, the sky model and antenna response modeling that emerge from the interferometer data would provide relatively poorer calibration of the mode coupling.

5.3 *Strategy 3*

Strategy 3 suggests a dedicated precision element in the form of an outrigger to each station and provide a wide-field auto-correlation signal, which would serve as the measurement set for the EoR science. These antennas may be designed to be wideband frequency-independent elements with relatively lower mode coupling (or multiple antennas, each optimized to operate over individual octave bands with appropriate offsets to span the full 50–350 MHz SKA-Low band). Even if the elements and station beams are frequency-independent, it may be mentioned here that the ionosphere could make the effective beam chromatic (Vedantham *et al.* 2014). It may be noted here that an outrigger placed sufficiently isolated from the station elements would escape inter-element coupling effects that are highly chromatic. LEDA has explored implementing this strategy for global CD/EoR detection using dedicated radiometer elements co-located with and well-spaced from the LWA interferometer (Price *et al.* 2018). The results from this combination of outrigger radiometers for global signal detection and an interferometer for power spectrum detection/measurement is awaited and

is expected to inform future implementations, such as those suggested herein.

The detection and mitigation of RFI will be far superior in all-sky measurements based on auto-correlation spectra of SKA-Low stations, which simultaneously record interferometer data. The SKA-Low baselines between the core stations are relatively small in wavelength units, and hence, RFI is poorly rejected in the interferometer integration times. Therefore, the visibilities are excellent detectors of RFI, particularly when Stokes V visibilities are formed, and constitute a calibration set for RFI recognition in time-frequency space that may be used to reject RFI-corrupted station signals. Moreover, interferometer data that do not contain the uniform all-sky signal may also be used to model and subtract RFI from the station's total power spectra, which constitute the measurement set. Real-time RFI rejection and mitigation algorithms that clean the SKA-Low station autocorrelation spectra using visibility data is desirable.

5.4 *Calibration for global CD/EoR with SKA*

Bandpass calibration of spectral radiometer elements that form SKA-Low interferometers may be done using spectral visibilities to solve sky structure and element gains simultaneously. While not applicable to Strategy 1, a purpose built complex calibration scheme (as routinely employed in dedicated single instrument global CD/EoR experiments) may be included in Strategies 2 and 3. This entails injection of flat-spectrum noise power via directional couplers for bandpass calibration that requires noise sources and couplers in every radiometer element. An alternate engineering solution for bandpass calibration of the radiometers is pulse calibration, which is the time domain equivalent of flat spectrum noise injection. By measuring the system response to pulses, much narrower than the inverse of the bandwidth, the bandpass calibration is derived. Different modes in the observed spectra may be tagged to reflections from different impedance discontinuities in the signal path. Yet another method for bandpass calibration is the injection of a swept frequency tone into the system path. In addition to bandpass calibration and the marginalization of additives, precision polarimetric calibration to estimate the unwanted confusing leakages from the polarized structure in the sky to spectral modes is necessary. Linearly polarized sky emission will appear with spectral structure in total power spectra of linearly polarized antenna elements if Faraday rotation changes the plane of polarization arriving at the antenna over frequency. Improper instrumental calibration along with Faraday rotation that causes the polarized signal to have frequency structure might confuse the all-sky EoR signature. In this context, once again, we see the advantage of using the SKA-Low for all-sky CD/EoR signal detection because of the ability of an interferometer array also to yield solutions for precision polarimetric calibration for the interferometer elements, which in this case constitute the spectral radiometers that measure the all-sky 21-cm signature. Specifically, Faraday rotation measure (RM) synthesis using interferometer visibilities offers a more complete and hence, accurate polarimetric calibration, associating each pixel in the sky with Stokes I along with (Q, U, RM) sets and their spectral indices. The Stokes V data are also useful in setting the thermal noise level apart from providing an indicator for radio frequency interference. The off-axis polarization effects are smaller in Strategy 1, which uses a narrow station beam of 5°, compared to Strategies 2 and 3, which use single antennas with broad beams as basic elements.

6. Outrigger antennas for SKA

The preferred strategy of using a separate array of outrigger antennas with SKA-Low for global CD/EoR signal detection is described here. The advantage of introducing outrigger antennas is that they could be customized or purpose-designed to have features necessary specifically for the detection of the global CD/EoR signal, which is not part of the current design specifications for SKA-Low stations as phased arrays or part of the design of SKA-Low log-periodic antennas. The outrigger antennas would be designed to be dual-polarized and wideband with frequency-independent radiation patterns and smoothly varying reflection coefficients. Most importantly, the new outriggers would be outfitted with precision self-calibratable receivers that would make their auto-correlation spectra of science quality. It is to be noted here that antennas that are frequency-independent over large bandwidths generally have broad beams (such as a short dipole).

When using outrigger antennas with SKA-Low, the auto-correlations of both polarization signals (X and Y) from each of the outriggers serve as the measurement set for global CD/EoR signal detection. The full Stokes correlations (XX, YY, XY and YX) between all elements in the array consisting of outriggers and SKA-Low stations together, serve as the calibration set. By having 64 outrigger antennas in SKA-Low (half of the

initial number of stations in the commissioning phase), a minimal modification to the current design of the SKA-Low correlator will get the required correlations. Thus, signals from the outriggers would simply take the place of those coming from the outer stations of SKA-Low, when observing for this science use case. The outriggers would, of course, have to be located with SKA-Low, so that the high sensitivity in baselines between outriggers and SKA-Low stations would provide the necessary calibration products for the precision calibration of the beam patterns, element gains, bandpass and polarization leakages of the outriggers. Placing the outrigger antennas in a compact array at the core of SKA-Low also offers the advantage of restricting calibration data for the global CD/EoR detection to baselines that are not severely affected by ionosphere; therefore, calibrations may be derived with greater accuracy.

It is not necessary to place an outrigger antenna with each SKA-Low core station. It is, in fact preferable to have an ultra-compact array of the outrigger antennas in the SKA-Low core area because this provides the added benefit of providing zero and short-spacings to image the large angular scale sky structures, adding baselines, which are not currently part of the SKA-Low design. This adds valuable information to the Global Sky Model derived from SKA-Low stations alone, making the data products from SKA-Low continuum surveys of higher fidelity.

Using outrigger antennas with SKA-Low for global CD/EoR signal detection will undoubtedly require the development of several new pipelines for precision polarimetric calibration of outriggers. The calibration data products from SKA-Low and outriggers, are the (i) multi-channel visibilities measured between SKA-Low stations, (ii) multi-channel visibilities measured between SKA-Low stations and outriggers, and (iii) multi-channel visibilities measured between outriggers.

The standard high dynamic range full polarization imaging pipeline would process the multi-channel visibilities measured between SKA-Low stations to generate the Global Sky Model. It may be noted here that useful closure phase and amplitude may be defined from four independent heterogeneous baselines between any two SKA-Low stations and any two outriggers. Additional algorithms and special pipelines would need to be developed to process the multi-channel visibilities measured between outriggers and SKA-Low stations and those between the outriggers themselves to obtain precise gain/bandpass/leakage calibration and primary beam patterns of the outrigger antennas.

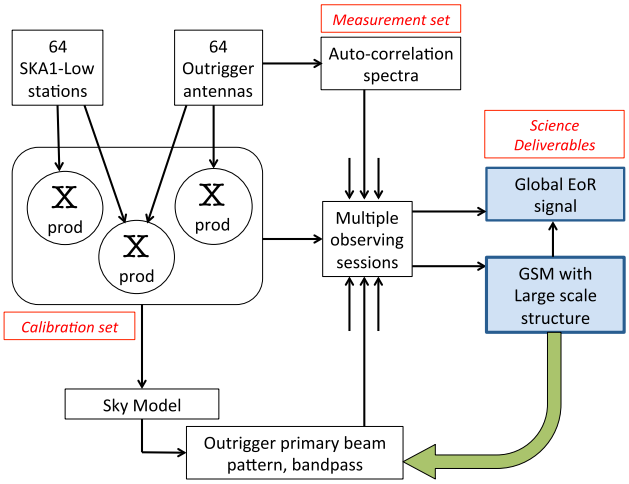

Figure 2. A block diagram showing the measurement set, calibration set and the resulting science deliverables, summarizing the strategy to detect global CD/EoR signal with the outrigger antennas in SKA-Low.

The primary beams of SKA-Low stations are narrow compared to the broad beams of the outrigger antennas; therefore, calibration over the wide outrigger beams needs observing with many pointings of SKA-Low stations. Observations may achieve this, in drift scan mode over a set of sessions in which SKA-Low stations are phased towards different directions spanning the meridian. Combining such data observed over several sessions also requires a custom-designed pipeline. The autocorrelation spectra of the outrigger antennas measured over several days along with the precisely calibrated bandpasses and primary beam patterns are used to extract the global CD/EoR signal.

A simple block diagram showing the measurement set, calibration set and the resulting science deliverables, summarizing the strategy to detect global CD/EoR signal with the outrigger antennas in SKA-Low, is given in Figure 2.

As a useful corollary, the short-baselines between the outrigger antennas in the ultra-compact array also image large-scale sky structures that are beyond the present imaging capability of SKA-Low. This will add significant scientific value to the Global Sky Model generated by SKA-Low.

Pilot observations, which could lead to useful science, may begin early in the commissioning phase with SKA-Low core stations. Useful measurement and calibration data-sets can be obtained once interferometer imaging, to solve for the Global Sky Model, is available, along with the required hardware and system calibration pipelines.

7. Outrigger antenna implementation checklist

To implement outrigger antennas to achieve the expected science returns, we anticipate the following steps. These are in no way exhaustive, but certainly essential.

1. Design and development of outrigger antennas and associated receiver electronics.
2. Design of the array configuration for outriggers and their placement relative to the SKA-Low core stations.
3. Signal transport considerations for carrying outrigger signals to the central correlator building.
4. Interface between the outrigger signals and SKA-Low correlator.
5. Enabling a new operational mode in the SKA-Low correlator to derive the measurement and calibration data sets.
6. An assessment of data acquisition rates and procurement of storage requirements.
7. Pipelines to process the measurement and calibration data sets to produce the science deliverables (global CD/EoR signal and GSM with large scale structure).

8. Path to SKA detection of primordial recombination lines

Another cosmological signal in the all-sky mean spectrum of the cosmic radio background is recombination lines from the epoch of recombination (Sunyaev & Chluba 2009). In contrast to the 21-cm signatures of reionization, the predictions of the recombination spectrum are rather precise, assuming standard recombination physics, and hence, serve as an excellent test of the standard model. These 'primordial recombination lines' are expected to appear as an extremely weak ripple in the cosmic radio background. They are predicted to be present across all SKA bands. Their detection is likely best done at centimeter wavelengths, where the signal-to-noise is expected to be greatest considering the line intensities, background sky noise contribution to measurement errors and receiver technology (Sathyanarayana Rao *et al.* 2015). The all-sky recombination spectral signature requires ∼100 spectral radiometers operating in parallel, and whose calibrated spectra are co-added, for detection in reasonable time.

With SKA however, the optimum frequency range for a signal detection is at the top of the SKA-Mid, band which provides a contiguous coverage between bands 5a and 5b over 4.6–15.8 GHz. The additive intensity from recombination to the CMB spectrum over this frequency range is shown in Figure 3. Once again, as in the case of CD/EoR detection with SKA-Low, the total power spectra of the dish elements that form the SKA-Mid interferometer form the measurement set for all-sky primordial recombination science.

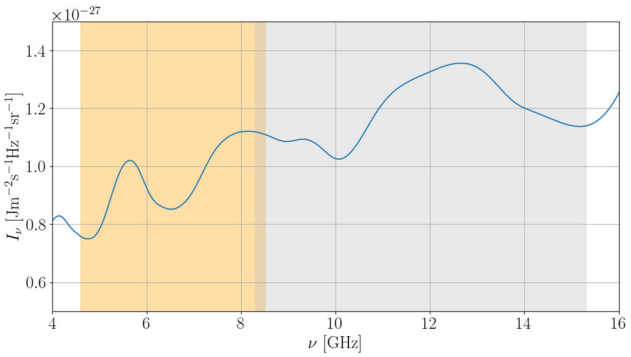

Figure 3. Total additive intensity spectrum from primordial recombination lines of hydrogen and helium to the CMB over the contiguous SKA-Mid bands 5a (orange) and 5b (grey). Data courtesy: Chluba & Ali-Haimoud (2016).

SKA-Mid elements operating as spectral radiometers is perhaps the only instrument capable of detecting these features in the foreseeable future; as discussed above, their operation as interferometers provides the calibrations for element bandpass and gains as well as solutions for mode coupling. A genuine attempt at a detection of the recombination spectrum is reserved for the full SKA, after completion of SKA-Mid in phase 2. Long duration imaging campaigns, perhaps as a deep all-sky survey, would yield the data set that might serve for detection of the recombination line signature with SKA-Mid in phases 1 and 2. All the discussions on the requirements for interferometer-based calibration of element bandpass in Section 5.4, and solving for the mode coupling of sky structure to spectral structure from continuum radio sources as well as linearly polarized emission along with Faraday rotation, are also relevant to SKA-Mid for detection of recombination lines. The SKA-Mid antennas are dishes that form the interferometer elements. Their autocorrelation spectra form the measurement set for the detection of recombination lines and hence, the additives in these signals will require calibration. Dish-type antennas are electrically large structures and hence, would have long lengths in the signal path arising from reflections off structural elements. For this reason, for the all-sky science, it is desirable for the dishes to be off-axis reflector antennas.

9. Summary

We have suggested several strategies to detect the global signal from CD and EoR with the SKA. Of these, a preferred strategy is placing a compact array of 64 dual polarized, frequency-independent and wideband outrigger antennas in the core of SKA-Low (phase 1). These precision outriggers would be fitted with self-calibratable receivers. In this configuration, the outrigger signals replace signals from SKA-Low stations outside the core, thus allowing the use of SKA-Low correlator with minimal enhancements. If implemented as an engineering change, the SKA-Low correlator would measure autocorrelation spectra of the outrigger antennas and the cross-correlations of the outriggers among themselves and with SKA-Low stations, in addition to the cross-correlations between SKA-Low core stations.

Processing of these data products requires specialized calibration software pipelines to obtain bandpass calibration and beam patterns of the outriggers. In a set of observing sessions made with meridian offsets in the narrow beams of SKA-Low stations, the broad beams of outriggers would be imaged in full, resulting in both models for the entire 3-D primary beam patterns of outriggers as well as for the global sky. These calibration products would be used to estimate the global CD/EoR signal from the autocorrelations of outriggers.

A significant by-product of such an outrigger array would be imaging large scale structures with the compact array of outriggers and providing an absolute offset and accurate scale for imaging surveys with SKA-Low. These are beyond the currently planned capability.

In summary, we have presented a concept of adding an ultra-compact array of very small precision calibrated antennas as a supplement to the SKA-Low interferometers, which will provide the missing zero-spacing and large-scale view of the sky and thereby improve fidelity and science value of imaging surveys. Most importantly, this very small array provides for global CD/EoR signal detection with SKA-Low.

10. Closing remarks: SKA-Low detection of all-sky 21-cm signal from CD/EoR

It is often the case that effective use of a complex experimental system for a key science goal for which it is custom-built, requires a deep understanding of performance and systematics, which requires experience with the instrument and development of appropriate calibration methods in the commissioning phase. New telescopes that push frontiers of technology come with surprises beyond the imagination of its designers and builders. The sensitivity of a spectral radiometer to the all-sky EoR signature is independent of collecting area and depends on the system temperature and integration time. Pilot observations, which could lead to useful science, could begin early in the commissioning phase with 128 stations once interferometer imaging is enabled to solve for the Global Sky Model and system calibration. The expected system temperature at 110 MHz is about 800 K and this leads to the nominal requirement of about 1 h observing time with 128 station beams to achieve 1 mK sensitivity with a 1 MHz bandwidth. The actual time required to achieve this sensitivity would be a factor of a few larger because of various switching schemes that are inevitably introduced for calibration. For example, EDGES has a three-way switching scheme, while SARAS cycles through six states of the receiver to obtain measurement and calibration data products. The above bandwidth and sensitivity are adequate to characterize the turning points in the spin temperature evolution curve (Figure 1). The advantage as the build out progresses towards completion of SKA-Low phase 1 is not in thermal noise-related sensitivity to all-sky EoR signal, but in increasing accuracy of the calibration of the individual radiometer elements. It may be noted here that the foregrounds are of substantially greater brightness towards longer wavelengths since the cosmic radio background has a steep $T_b \propto \nu^{-2.5}$ dependence on frequency; therefore, successful imaging of the spatial structure in 21-cm spin flip is increasingly challenging towards earlier times in the evolution of the gas. The substantially greater calibration accuracy and confusion subtraction required for elucidating early-time evolution through interferometer imaging encourages designing for first detecting the wideband all-sky signature, which may be done in SKA-Low phase 1. All-sky detection of the absorption trough will serve as a motivation and prelude to later imaging of the spatial structure. The experience with SKA-Low phase 1 would be critical to the design of the elements of the SKA-Low phase 2, in design of the antenna elements and calibration schemes for additives.

References

Abdurashidova Z., Aguirre J. E., Alexander P., *et al.* 2022, The Astrophysical Journal, 925, 221

Bernardi G. 2017, Proceedings of the International Astronomical Union, 12, 98

Bernardi G., McQuinn M., Greenhill L. J. 2015, The Astrophysical Journal, 799, 90
Bowman J. D., Rogers A. E. E., Monsalve R. A., Mozdzen T. J., Mahesh N. 2018, Nature, 555, 67
Chluba J., Ali-Haimoud Y. 2016, Monthly Notices of the Royal Astronomical Society, 456, 3494
Cohen A., Fialkov A., Barkana R., Lotem M. 2017, Monthly Notices of the Royal Astronomical Society, 472, 1915
Datta K. K., Ghara R., Hoque A., Majumdar S. 2022, Monthly Notices of the Royal Astronomical Society, 509, 945
de Lera Acedo E. 2019, in 2019 International Conference on Electromagnetics in Advanced Applications (ICEAA), IEEE, 0626
Fialkov A., Barkana R. 2014, Monthly Notices of the Royal Astronomical Society, 445, 213
Field G. B. 1958, Proceedings of the IRE, 46, 240
Field G. B. 1959, The Astrophysical Journal, 129, 536
Furlanetto S. R., Oh S. P., Briggs F. H. 2006, Physics Reports, 433, 181
Koopmans L., Pritchard J., Mellema G., *et al.* 2015, in Proceedings of Advancing Astrophysics with the Square Kilometre Array—PoS(AASKA14), Vol. 215, 001
Liu A., Parsons A. R. 2016, Monthly Notices of the Royal Astronomical Society, 457, 1864
Madau P., Meiksin A., Rees M. J. 1997, The Astrophysical Journal, 475, 429
McGreer I. D., Mesinger A., D'Odorico V. 2015, Monthly Notices of the Royal Astronomical Society, 447, 499
McQuinn M. 2016, Annual Review of Astronomy and Astrophysics, 54, 313
Mellema G., Koopmans L. V. E., Abdalla F. A., *et al.* 2013, Experimental Astronomy, 36, 235
Mertens F. G., Mevius M., Koopmans L. V. E., *et al.* 2020, Monthly Notices of the Royal Astronomical Society, 493, 1662
Meys R. 1978, IEEE Transactions on Microwave Theory and Techniques, 26, 34
Monsalve R. A., Rogers A. E. E., Bowman J. D., Mozdzen T. J. 2017, The Astrophysical Journal, 835, 49
Morales M. F., Wyithe J. S. B. 2010, Annual Review of Astronomy and Astrophysics, 48, 127
Nambissan T., J., Subrahmanyan R., Somashekar R., *et al.* 2021, Experimental Astronomy, https://doi.org/10.1007/s10686-020-09697-2
Nhan B. D., Bordenave D. D., Bradley R. F., *et al.* 2019, The Astrophysical Journal, 883, 126
Offringa A. R., de Bruyn A. G., Biehl M., *et al.* 2010, Monthly Notices of the Royal Astronomical Society, 405, 155
Pal S., Bharadwaj S., Ghosh A., Choudhuri S. 2021, Monthly Notices of the Royal Astronomical Society, 501, 3378
Peebles P. J. E. 1993, Principles of Physical Cosmology, Vol. 27 (Princeton University Press)
Price D., Greenhill L., Fialkov A., *et al.* 2018, Monthly Notices of the Royal Astronomical Society, 478, 4193
Pritchard J. R., Loeb A. 2008, Physical Review D, 78, 103511
Pritchard J. R., Loeb A. 2010, Physical Review D, 82, 023006
Pritchard J. R., Loeb A. 2012, Reports on Progress in Physics, 75, 086901
Sathyanarayana Rao M., Subrahmanyan R., Udaya Shankar N., Chluba J. 2015, The Astrophysical Journal, 810, 3
Sathyanarayana Rao M., Subrahmanyan R., Udaya Shankar N., Chluba J. 2017, The Astrophysical Journal, 840, 33
Seager S., Sasselov D. D., Scott D. 2000, The Astrophysical Journal Supplement Series, 128, 407
Singh S., Subrahmanyan R., Shankar N. U., *et al.* 2018, Experimental Astronomy, 30
Singh S., Nambissan T., Subrahmanyan R., *et al.* 2022, Nature Astronomy, 6, 607
Subrahmanyan R., Shankar N. U., Pritchard J., Vedantham H. K. 2015, arXiv preprint 1501.04340
Sunyaev R. A., Chluba J. 2009, Signals from the epoch of cosmological recombination–Karl Schwarzschild Award Lecture 2008
Vedantham H. K., Koopmans L. V. E., de Bruyn A. G., *et al.* 2014, Monthly Notices of the Royal Astronomical Society, 437, 1056
Wouthuysen S. A. 1952, The Astronomical Journal, 57, 31
Yoshiura S., Pindor B., Line J. L. B., *et al.* 2021, Monthly Notices of the Royal Astronomical Society, 505, 4775
Zaroubi S. 2013, The First Galaxies, 396, 45